energy&fuels

Article

pubs.acs.org/EF

Biodiesel Fuels from Supercritical Fluid Processing: Quality Evaluation with the Advanced Distillation Curve Method and Cetane Numbers

George Anitescu* and Thomas J. Bruno*

Thermophysical Properties Division, National Institute of Standards and Technology, Boulder, Colorado 80305, United States

ABSTRACT: The volatility of biodiesel fuel samples produced by supercritical (SC) transesterification (TE) of triglyceride feedstocks of chicken fat and soybean oil was determined by the advanced distillation curve (ADC) method. Particularly high temperatures (e.g., 400 °C) of the SCTE process partially decomposed the polyunsaturated fatty acid methyl esters (FAMEs) to lower molecular FAMEs (~C_6–C_{15}) and ~C_{10}–C_{17} hydrocarbons. These lighter fuel components shifted the first portion of the distillation curves toward that of #2 diesel fuel. This means that biodiesel fuels produced by SCTE at ~400 °C exhibit higher overall volatility when compared to commercial biodiesel samples produced by conventional catalytic TE. Other important fuel properties such as ignition delay via cetane numbers could also be improved. This information will permit efficient fuel system and combustion chamber designs to optimize fuel utilization in diesel engines, decrease of fuel consumption, and emission mitigation.

INTRODUCTION

Among alternative renewable fuels produced from biomass (i.e., biofuels) to extend and enhance petroleum-derived fuels, biodiesel fuel is already on an appreciable scale of commercial production due to the availability of various triglyceride feedstocks such as vegetable oils and animal fats.[1−9] However, along with feedstock cost, the conventional conditions of lipid transesterification (TE) reactions render this fuel more expensive than its counterpart, petroleum-derived diesel fuel (PDDF).[7,10,11] The problem resides in carrying out these reactions under nonoptimized conditions, resulting in complex mixtures of residual reactants, catalysts, reaction products, and byproducts, followed by tedious separation and purification steps. Furthermore, some of the important properties of commercial biodiesel fuels are inferior to those of PDDFs.[1] Among these properties are volatility, cold flow behavior, viscosity, and storage stability (chemical reactivity at ambient conditions).

Alternative processes to carry out cost-effective TE reactions of various feedstocks, such as supercritical TE (SCTE), require reactant properties over an extended range of thermodynamic conditions, particularly mutual solubilities at temperatures of preheated reactants.[2−7,10−14] Obviously, triglyceride−alcohol reactants in a single, homogeneous phase will lead to the fastest and most complete reactions. As an important advantage, in the supercritical (SC) phase at approximately 350−400 °C, the byproduct glycerol thermally decomposes or reacts with the excess alcohol to form valuable fuel components.[5,10−14] Also, contrary to the conventional impression in fuel research, SCTE temperatures of 350−400 °C will not be detrimental to fuel quality by the partial decomposition of FAMEs. The polyunsaturated FAMEs are consumed to generate lower molecular FAMEs and hydrocarbons that will improve the fuel quality, as shown in previous studies[10−14] and herein.

The fatty acid composition of a biodiesel fuel generally corresponds to that of its parent oil or fat. Thus, biodiesel fuels derived from different sources can have significantly varying fatty acid profiles and properties.[1,15] The most common fatty esters contained in a commercial biodiesel fuel are those of palmitic, stearic, oleic, linoleic, and linolenic acids. While some of these esters confer desired properties to the fuel, others exhibit opposite effects. The volatility of these high molecular mass esters is relatively low, but this increases significantly with a decrease in the molecular size caused by chemical reactions. The cetane number, related to the ignition quality of a diesel fuel, decreases with a decreasing molecular chain length and an increasing unsaturation of the fatty acids.[16] Saturated esters have (desirable) high cetane numbers but lower volatility, while unsaturated, especially polyunsaturated, fatty esters have low cetane numbers and reduced oxidative stability but lower melting points that are desirable for a biodiesel fuel.[15−17]

Solutions to improve one of these properties often increase undesirable behavior of another property.[15] To mitigate the effect of a variable fatty acid profile on biodiesel fuel properties, simultaneous thermal reactions with those of SCTE are potentially beneficial. Such reactions occur in the process of SCTE carried out at higher temperatures (e.g., approximately 400 °C).[10−13] Among the reaction products are smaller molecular esters (C_6 to C_{15}) and hydrocarbons (C_{10} to C_{17}), both saturated and unsaturated. These fuel components improve the less favorable properties of biodiesel fuels such as cold flow behavior, viscosity, cetane numbers, and volatility.

Most incremental advancements on diesel engine efficiency and emission mitigation have been focused on the engine itself (e.g., high-performance fuel systems, combustion chamber architecture, turbocharging, EGR, etc.).[18] There is significant opportunity for breakthroughs and improvements, by focusing on the fuel as well.[19−22] While diesel engines are robust power

Received: April 11, 2012
Revised: June 29, 2012
Published: July 9, 2012

plants working with various fuels, the conventional way of delivering these fuels to combustion chambers as liquid droplets at low temperature can be improved and deserves additional inquiry. Indeed, the main problem of engine efficiency and pollution is the fact that these droplets do not have enough time to first vaporize, and then mix and react with the air in a short engine thermodynamic cycle. Alternative methods to the conventional combustion are being focused on heated fuels[21,22] as well as new diesel−biodiesel blends.[23,24] Modeling fuel combustion in diesel engines requires reliable fuel property data such as volatility, heat capacity, density, diffusivity, critical point, surface tension, and viscosity over wide ranges of $P-V-T-x$ conditions.[5] The distillation (or boiling) curve of a complex fuel such as biodiesel is a critically important indicator of the bulk behavior of the fuel. For this reason, the distillation curve is often cited as a primary design and testing criterion for liquid fuels.[24−30]

In this study, volatilities of the biodiesel fuel produced by the SCTE method and those of two blends with #2 diesel fuel were determined by the advanced distillation curve method.[5,31−34] The work on the title topic was performed on two SCTE biodiesel fuel samples[10,13] and on two samples of commercial biodiesel fuels produced by a conventional catalytic TE method. The two SCTE biodiesel fuel samples were produced at 400 °C from chicken fat and soybean oil in reactions with methanol and showed improved properties in previous studies.[10−13]

EXPERIMENTAL SECTION

Materials. Two samples of biodiesel fuels were produced from refined soybean oil and rendered chicken fat in a laboratory-scale reactor at SCTE conditions (400 °C with an uncertainty of 5 °C, 10 MPa with an uncertainty of 0.1 MPa, 9:1 methanol to lipid molar ratio, and 5−9 min residence time).[10,13] Another sample of biodiesel fuel, produced by catalytic TE, was obtained from a commercial supplier. The biodiesel fuel samples were subjected to chemical analysis before the measurement of the distillation curve. They were analyzed with gas chromatography with mass spectrometric detection, GC-MS, (in scanning mode) with a 30 m capillary column with a 0.1 μm coating of the stationary phase, 50% cyanopropyl−50% dimethyl polysiloxane. This stationary phase provides separations based upon polarity and is specifically intended for the analysis of the FAME compounds that make up biodiesel fuels.[35,36] Peaks were identified with guidance from the NIST/EPA/NIH Mass Spectral Database, and also on the basis of retention indices.[37] The *n*-hexane used as a solvent in this work was obtained from a commercial supplier and was analyzed by gas chromatography (30 m capillary column of 5% phenyl−95% dimethyl polysiloxane having a thickness of 1 μm, temperature program from 50 to 170 °C at a heating rate of 5 °C per minute) with flame ionization and mass spectrometric detection. These analyses revealed the purity to be approximately 99%, and the fluid was used without further purification.

Apparatus. The volatility of biodiesel fuels was determined by the advanced distillation curve method, which has been used in the past on biodiesel fuels.[24,29,30,38] The method and apparatus for ADC measurements have been reviewed in detail elsewhere.[25,26,39−42] In brief, a 50 mL aliquot of biodiesel fuel was placed into a boiling flask for each measurement. Two thermocouples were inserted into the proper locations to monitor T_k (the temperature in the liquid phase) and T_h (the temperature at the bottom of the takeoff position in the distillation head). Enclosure heating was then started with a four-step program based upon a previously measured distillation curve. Volume measurements were made in graduated cylinders with readings of 0.1 mL, and one drop of the distilled liquid sample was collected in a GC vial of 1.5 mL for each volumetric fraction distilled. Since oxidative degradation of the FAME components of biodiesel fuel is known to occur during atmospheric pressure measurements, we placed a sparge tube into the distillation kettle and bubbled argon into the liquid phase for 10 min with stirring before applying heat.[24] After 10 min, the sparge tube was removed from the liquid to avoid affecting the fluid temperature during the distillation, but argon purge of the atmosphere above the liquid phase was maintained throughout the distillation at a flow rate of 1 mL/min.

The average experimental atmospheric pressure for the ADC measurements presented herein was 83.1 kPa, with an uncertainty of 0.003 kPa. The usual pressure adjustments of these measurements to a sea-level atmospheric pressure of 101.325 kPa were not applied in this work because our purpose was to compare the volatility of the biodiesel fuels obtained by different methods. The use of the adjusted pressure will leave the shapes of the distillation curves unchanged but will result in a typical temperature increase of ∼8 °C.

The measurement of distillation curves provided temperature, volume, and composition-explicit data that allowed qualitative and quantitative analyses of each fraction of the distillation. The fuel composition, the most important underlying parameter that governs curve shape, was determined for samples of fuels obtained by SCTE of soybean oil and chicken fat[10,13] and compared to those of commercial biodiesel fuels and #2 diesel fuel. The measurements were performed in replicate (with between three and six individual measurements); thus, the averaged values are reported. The combined uncertainty (including repeatability and the calibration) of the temperature measured in the liquid phase was 1.94, 2.94, and 2.73 °C for the biodiesel fuel samples from soybean, chicken fat, and commercial source, respectively.

Analytical Method. The methyl ester content in the biodiesel fuel samples was determined by a gas chromatograph (GC) with mass selective detector (MSD) containing a cross-linked capillary column with 0.15 μm coating of 50% cyanopropyl−50% dimethyl polysiloxane (30 m × 0.25 mm inner diameter (i.d.) × 0.15 μm film thickness). Helium was used as carrier gas at a split ratio of 100:1 with constant head pressure of 69 kPa. The temperature program began at 80 °C (hold for 2 min) and continued with a subsequent ramp of 5 °C/min to 220 °C (hold for 5 min). The temperatures of the injector and GC−MSD interface were 350 and 250 °C, respectively. The stationary phase, specifically intended for the analysis of the polar compounds that make up biodiesel fuels, provided separation based upon boiling temperature and polarity. Mass spectra were collected for each peak from 15 to 550 relative molecular mass (RMM, formerly Daltons or amu) units. Peaks were identified with guidance from the NIST/EPA/NIH Mass Spectral Database, and also on the basis of Kovats retention indices.[37] Only the peaks with areas >3% of the area of the largest peak in each chromatogram were considered. The average mole fraction uncertainty in the chemical composition was 2.6% and was propagated from the area repeatability on the chromatograms and calibration measurements.

For the analysis of biodiesel fuel blended with diesel fuel, a capillary column with 5% phenyl polydimethyl siloxane (30 m × 0.25 mm i.d. × 0.25 μm film thickness) was used. The temperature program was from 60 °C (hold for 2 min) to 180 at 3 °C/min and then to 290 at 6 °C/min. Injector temperature was 300 °C, the split ratio 100:1, and the transfer line temperature was 280 °C.

RESULTS AND DISCUSSION

FAME Characterization. Saturated and unsaturated FAMEs obtained from various triglyceride feedstocks exhibit different properties that significantly affect the fuel quality.[15,16] The molecular length of fatty acids as constituents of FAMEs considerably affects the fuel properties, especially volatility, viscosity, and cold flow behavior, as well as the cetane number of the fuels. The fatty acid patterns of the soybean oil and chicken fat[13,43] used to produce biodiesel fuels (Table 1) are not significantly affected by preheating these feedstocks up to ∼350 °C.[10,12,13] However, during SCTE reactions carried out at approximately 400 °C, thermal decomposition of the

dx.doi.org/10.1021/ef300615r | Energy Fuels 2012, 26, 5256−5264

Table 1. Fatty Acid Profile (%, mass/mass) for Chicken Fat and Soybean Oil and Normal Boiling Temperature, T_b[a], of the Corresponding FAMEs at 83 kPa[b]

fatty acid	chicken fat[13]	soybean oil[43]	FAME normal T_b[29]
palmitoleic	7.7	0.7	316.9
palmitic	21.0	14.1	319.8
stearic	5.5	5.2	346.8
oleic	48.5	25.3	344.6
linoleic	17.3	48.7	345.9
linolenic	traces	6.1	346.9
unsaturated	73.5	80.8	
saturated	26.5	19.3	

[a]the uncertainty of T_b measurement is 0.3 °C. [b]Additional details on the measurements and uncertainty can be found in the cited references.

unsaturated FAMEs takes place. Previous studies have reported that the molecular size and degree of unsaturation have a strong impact on the thermal stability of the FAMEs at high temperatures.[10−13,44,45] The double bonds act as weak links in the FAME chains, leaving them more susceptible to cleavage and, thus, creating shorter FAMEs and *n*-alkanes/alkenes. There is also evidence supporting a polymerization type reaction that creates heavier products at high temperatures.[46,47]

GC-MSD chromatograms of the biodiesel fuel samples obtained by SCTE at 400 °C show a concentration of esters (C_6−C_{15}) and hydrocarbons (C_{10}−C_{15}) of up to 4% (Figure 1, top). This content is negligible for the biodiesel fuel samples produced by a conventional catalytic TE process at low temperatures (Figure 1, bottom). Chemical compositions of the distilled fractions of SCTE-processed biodiesel fuel from chicken fat at 400 °C are compared to those of a commercial biodiesel fuel sample in Table 2. The composition of the commercial biodiesel fuel is unremarkable and agrees very well with several soy-derived biodiesel fuels previously analyzed.[36] The composition of the biodiesel fuels produced by SCTE[10,13] contained lower molecular mass FAMEs and hydrocarbons (both saturated and unsaturated) and less polyunsaturated FAMEs. Nevertheless, the main components that are expected in a biodiesel fuel were not significantly affected by the high SCTE temperatures, such as the methyl esters of palmitic, stearic, oleic, and linoleic acids; they are well preserved.

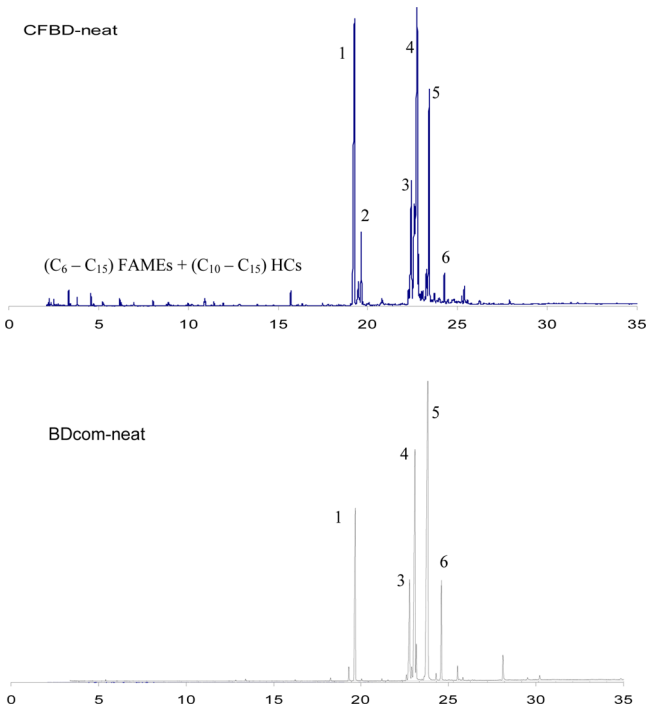

Figure 1. GC-MSD chromatograms of neat biodiesel fuel obtained by SC transesterification of chicken fat at 400 °C (top) and neat commercial biodiesel fuel (bottom). The peak numbers are the methyl esters of the (1) palmitic, (2) palmitoleic, (3) stearic, (4) oleic, (5) linoleic, and (6) linolenic acids.

Volatility of Neat Biodiesel Fuels (B100). The volatility of the biodiesel fuel samples was measured with the advanced distillation curve method (ADC). The measurements yielded thermodynamically consistent temperatures for each volume fraction, both in liquid and vapor phases. In Table 3, we give only the temperatures T_k recorded in the liquid phase. As shown in Figure 2, the distillation curves for neat biodiesel fuel samples were compared with the distillation curves of selected commercially available biodiesel and diesel fuels that are considered typical (e.g., soybean biodiesel fuel and #2 diesel fuel).

The experimental results show that renewable biodiesel fuel samples obtained from SCTE processing exhibit higher volatility compared to commercial biodiesel fuels produced by the conventional catalytic TE method. This volatility is very close to that of the #2 diesel fuel at the start of vaporization, while commercial biodiesel fuel starts boiling at a temperature that is higher by more than 100 °C. At the end of the distillation curves, biodiesel fuel samples obtained at 400 °C by SCTE showed no significant thermal decomposition. The distillation curve of the commercial biodiesel exhibits a sharp increase in temperature at volumetric fractions higher than ∼70% as a result of significant thermal decomposition or polymerization.

The differences in the distillation curves result from different chemical compositions of the biodiesel fuel samples studied, as shown earlier. As seen in Figure 3, the fuels undergo major compositional transformations during the distillation. Clearly, a gradual decrease of methyl linolenate and methyl linoleate is observed in samples from the 70% to the 80% distillate volume fraction as the distillation progresses. By the 80% fraction, nearly all the methyl linolenate has been depleted and much of the methyl linoleate has also been reduced at 90%. These two esters have the highest degree of unsaturation and decompose more easily as a result of their double bonds. Some fraction of the decomposition products are boiled off and can be seen in Figure 3 as the small peaks between 2 and 15 min retention times. Since methyl linoleate and methyl linolenate are multiunsaturated, the double bonds are also susceptible to polymerization by the Diels−Alder reaction.

Volatility of Biodiesel−Diesel Fuel Blends (B20 and B50). In addition to the neat biodiesel fuels, 20% (B20) and 50% (B50) blends of fuel samples from chicken fat processed under SC conditions with #2 diesel fuel were also studied. The distillation curves are shown in Figure 4, compared to those of the neat fuels (B100 and #2 diesel fuel). At the beginning of the distillation process, the distillation curves of the blends are close to that of #2 diesel fuel due to the more volatile components of the diesel fuel. As distillation progresses, these curves gradually depart the distillation curve of the diesel fuel and approach that of the biodiesel fuel.

dx.doi.org/10.1021/ef300615r | *Energy Fuels* 2012, 26, 5256−5264

Table 2. Chemical Compositions of the Distilled Fractions of SCTE-Processed Biodiesel Fuel from Chicken Fat at 400 °C Compared to Those of a Commercial Biodiesel Fuel Sample

	biodiesel fuel from chicken fat by SC transesterification								commercial biodiesel		
FAMEs/HCs	neat	1%	10%	30%	50%	70%	80%	90%	neat	1%	80%
$C_6H_{12}O_2$	0.06	2.28						1.23			
$C_6H_{10}O_2$	0.02	0.76						0.41			2.37
$C_7H_{14}O_2$	0.18	8.97						2.08			5.75
$C_7H_{12}O_2$	0.05	2.90						1.01			2.25
$C_8H_{16}O_2$	0.45	18.93					0.88	4.29		3.12	11.97
$C_8H_{14}O_2$	0.28	12.13						2.60			5.99
$C_9H_{18}O_2$	0.41	12.20					1.93	5.90		62.01	17.93
$C_9H_{16}O_2$	0.11	3.85						2.73			7.21
$C_{10}H_{20}O_2$	0.24	5.16					0.96	4.63			9.29
$C_{10}H_{18}O_2$	0.12	2.41						2.62			4.62
$C_{11}H_{22}O_2$	0.23	2.28					1.17	4.16			5.75
$C_{11}H_{20}O_2$	0.07	2.67						1.31			
$C_{12}H_{24}O_2$	0.09	0.77						1.67			
$C_{12}H_{22}O_2$	0.47	3.43						1.39			
$C_{13}H_{26}O_2$	0.08							1.03			
$C_{13}H_{24}O_2$	0.09							0.46			
$C_{14}H_{28}O_2$	0.05							0.74			
$C_{14}H_{26}O_2$	0.03							0.38			
$C_{15}H_{30}O_2$	0.49		1.43					0.94			
$C_{15}H_{28}O_2$	0.15							0.41			
$C_{16}H_{32}O_2$	0.08							0.76			
$C_{16}H_{30}O_2$	0.05							1.08			
$C_{17}H_{34}O_2$	23.01	2.40	39.78	35.64	27.85	19.56	14.71	11.74	13.34	8.35	
$C_{17}H_{32}O_2$	4.39		4.43	5.57	3.85	1.34	1.00	1.65			
$C_{18}H_{36}O_2$	0.16							0.48			
$C_{18}H_{34}O_2$	0.08							0.56			
$C_{19}H_{38}O_2$	7.63		6.57	7.54	9.71	12.81	15.42	8.52	8.62		12.18
$C_{19}H_{36}O_2$	36.12		34.44	38.07	45.53	54.45	50.06	7.30	25.92	3.48	
$C_{19}H_{34}O_2$	16.92		13.35	13.18	14.01	11.84	6.26	1.54	41.51	7.59	
$C_{19}H_{32}O_2$	2.00	0.79							6.47		
$C_{21}H_{42}O_2$	1.16							1.07			
$C_{22}H_{44}O_2$	0.28						0.98	1.04	0.81		
$C_{23}H_{46}O_2$	0.17						0.80	1.87	1.55		14.69
C11 (=)[a]	0.25	11.14						1.35			
C12 (−)[b]	0.04	0.65						0.76			
C12 (=)	0.08	1.27						0.78			
C13 (−)	0.05	0.95						1.03			
C13 (=)								0.86			
C14 (−)	0.07							1.39			
C15 (−)	0.08						0.90	2.73			
C16 (−)	0.06							1.10			
C17 (−)	0.04							1.82			
others	3.61	4.06					4.93	10.58	1.78	15.45	

[a](=) unsaturated *n*-alkenes (olefins). [b](−) saturated *n*-alkanes.

In Figure 5 we show a chromatographic sequence of the chemical composition variation during the distillation of the B20 blend with biodiesel fuel from SCTE of chicken fat. The composition of the 10% distilled fraction mainly consists of the most volatile components of diesel fuel, while the main FAME ester content is negligible. The chromatographic peaks of lower molecular mass FAMEs that distilled with the volatile components of diesel fuel are dwarfed by the peaks of the latter. As distillation progresses, the heavier components of diesel fuel are dominant along with the main FAMEs of the biodiesel fuel. Remarkably, the unsaturated FAMEs do not undergo significant thermal decomposition when blended with diesel fuel compared to the case of the B100 fuels. An inhibiting effect of the heavier components of diesel fuel toward unsaturated FAME decomposition could be a feasible explanation for this behavior. We have observed similar phenomena in our global reaction rate kinetics measurements[48−54] and we called this "collisional deactivation". The high temperature caused the more stable molecules to encounter the less stable molecules more frequently and de-energized those in an excited state that were ready to decompose.

For the sake of comparison with B20 containing biodiesel fuel from the SCTE of chicken fat, we show in Figure 6 a sequence of chromatograms of the distilled volumetric fractions from the B20 blend with commercial biodiesel fuel. Similar to

dx.doi.org/10.1021/ef300615r | Energy Fuels 2012, 26, 5256−5264

Table 3. Distillation Temperature Data[a] for SCTE-Processed Soybean and Chicken Fat Biodiesel Fuels Compared to Commercial Biodiesel and Diesel Fuels[b]

SCTE soybean biodiesel fuel		SCTE chicken fat biodiesel fuel		commercial biodiesel fuel		diesel fuel #2	
X_v	T_k (°C)	X_v	T_k (°C)	X_v	T_k (°C)	X_v	T_k (°C)
IBT	226.4	0.00	227.0	IBT	338.0	0.05	225.5
0.01	277.9	0.04	300.0	0.05	341.4	0.10	230.1
0.02	292.4	0.06	319.1	0.10	342.5	0.15	235.4
0.04	305.7	0.08	329.3	0.15	343.3	0.20	240.9
0.06	317.8	0.10	333.1	0.20	343.9	0.25	245.9
0.08	328.3	0.14	338.3	0.25	345.4	0.30	251.2
0.10	334.1	0.20	341.7	0.30	346.5	0.35	256.5
0.14	342.0	0.24	343.9	0.35	348.0	0.40	261.9
0.20	348.7	0.30	346.9	0.40	348.9	0.45	268.2
0.24	352.4	0.34	348.0	0.45	349.8	0.50	273.8
0.30	357.2	0.40	351.8	0.50	351.5	0.55	280.2
0.34	360.5	0.44	353.5	0.55	352.8	0.60	287.1
0.40	365.3	0.50	356.8	0.60	356.6	0.65	294.3
0.44	368.6	0.54	360.6	0.65	360.6	0.70	301.6
0.50	374.0	0.60	365.7	0.70	367.8	0.75	310.0
0.60	386.9	0.70	381.5	0.80	397.4	0.85	328.9
0.64	392.3	0.74	389.3	0.85	418.9		
0.70	399.4	0.76	394.9				
0.74	404.1	0.78	399.1				
0.76	406.1	0.80	404.3				
0.78	408.0	0.82	408.5				
0.80	411.3	0.84	412.0				
		0.86	415.2				
		0.88	418.0				
		0.90	423.0				

[a]The uncertainty of the temperature measured in the liquid phase was 1.94, 2.94, and 2.73 °C for soybean, chicken fat, and commercial biodiesel fuel samples, respectively. [b]The columns labeled X_i are the distillate volume fractions. IBT is the initial boiling temperature, measured as the vapor rise temperature during the ADC measurement.

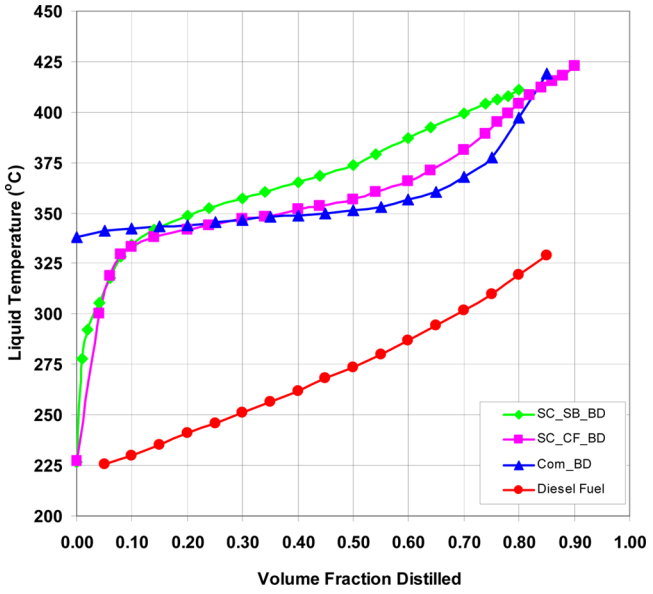

Figure 2. Distillation curves for biodiesel fuel samples obtained by supercritical transesterification of soybean oil (SC_SB_BD) and chicken fat (SC_CF_BD) with methanol compared to commercial biodiesel (Com_BD) and diesel fuel #2. The uncertainty of the temperature measured in the liquid phase was 1.94, 2.94, and 2.73 °C for soybean, chicken fat, and commercial biodiesel fuel samples, respectively.

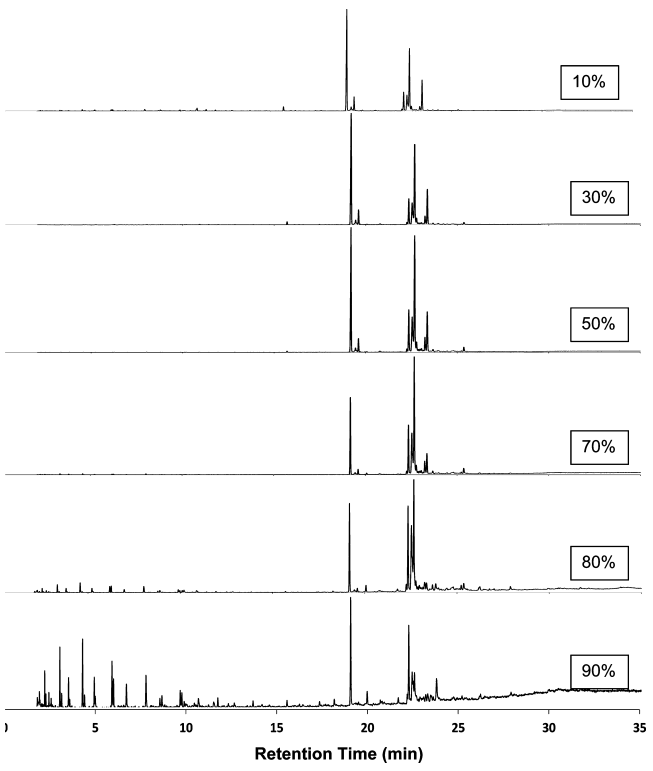

Figure 3. Composition evolution during distillation of SC CFBD with volumetric fraction.

the B20 blend with biodiesel fuel from SCTE of chicken fat, no significant thermal decomposition is observed as distillation progresses. As indicated in the discussion of Figure 5, this behavior originates from the protective effect of diesel fuel hydrocarbons against thermally labile FAMEs.

Cetane Numbers. The chemical compositions of the original biodiesel fuels and their distillation fractions are important in order to obtain various properties of interest in the complex process of modeling the fuel combustion. In this work, we discuss the cetane numbers of the biodiesel fuels, as shown in the next section. Cetane number is a relative ranking of fuels based on the period of time between fuel injection and ignition (i.e., ignition delay).[1,15,55] Fuels for compression ignition engines, including biodiesel fuel blends, must ignite through autoignition alone. The ability to rate the ignition quality of compression ignition fuels is important to diesel fuel formulation. Without adequate fuel ignition quality, the engine will start with difficulty and run poorly. Ultimately, the physical and chemical ignition delay of fuels is determined by the molecular structure of the fuel components and, thus, by fluid properties such as density, viscosity, surface tension, specific heat, enthalpy of vaporization, vapor pressure (volatility), vapor diffusivity, and chemical reactivity (energy of activation). Understanding how the molecular composition of fuels impacts ignition properties will lead to improved fuel formulations that enable higher efficiency engine operation.

As shown in Table 4, the cetane number of FAMEs increases with the molecular length and with chemical saturation. Accordingly, the lower molecular FAMEs produced by thermal

dx.doi.org/10.1021/ef300615r | Energy Fuels 2012, 26, 5256−5264

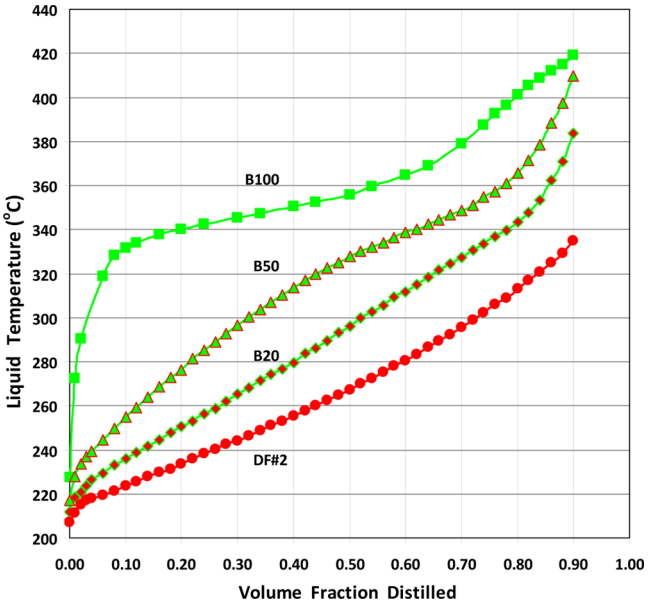

Figure 4. Distillation curves for blends of 20% (B20) and 50% (B50) biodiesel fuel (obtained by SCTE of chicken fat) in #2 diesel fuel (DF#2). The uncertainty of the temperature measured in the liquid phase was smaller than the size of the data-point symbols.

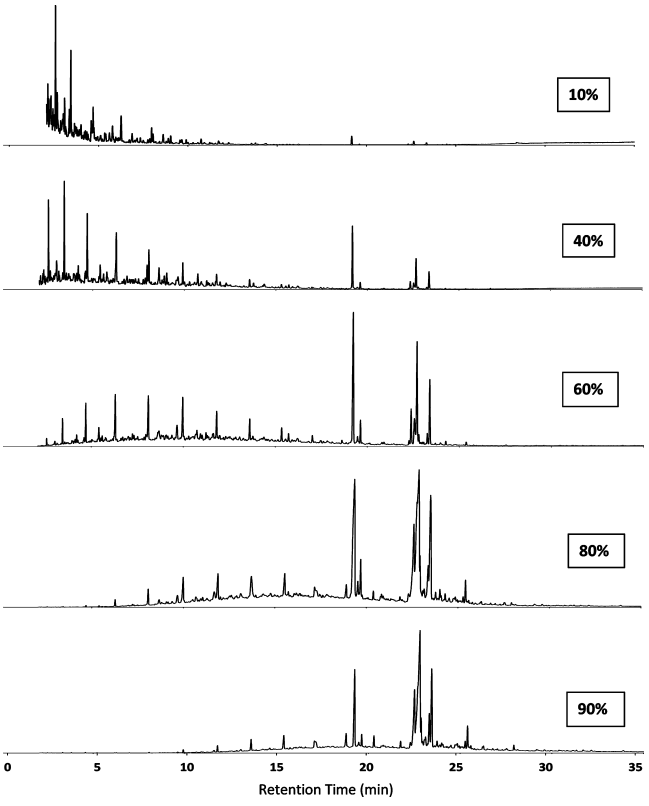

Figure 5. A sequence of the GC-MS chromatograms as function of the volume fraction distilled for diesel fuel−biodiesel fuel blends (20% vol/vol SCTE chicken fat biodiesel fuel).

decomposition of polyunsaturated, high molecular mass FAMEs, exhibit higher cetane number due to the higher level of saturation on one hand but lower cetane number, on the other hand, due to shorter molecular lengths. With respect to

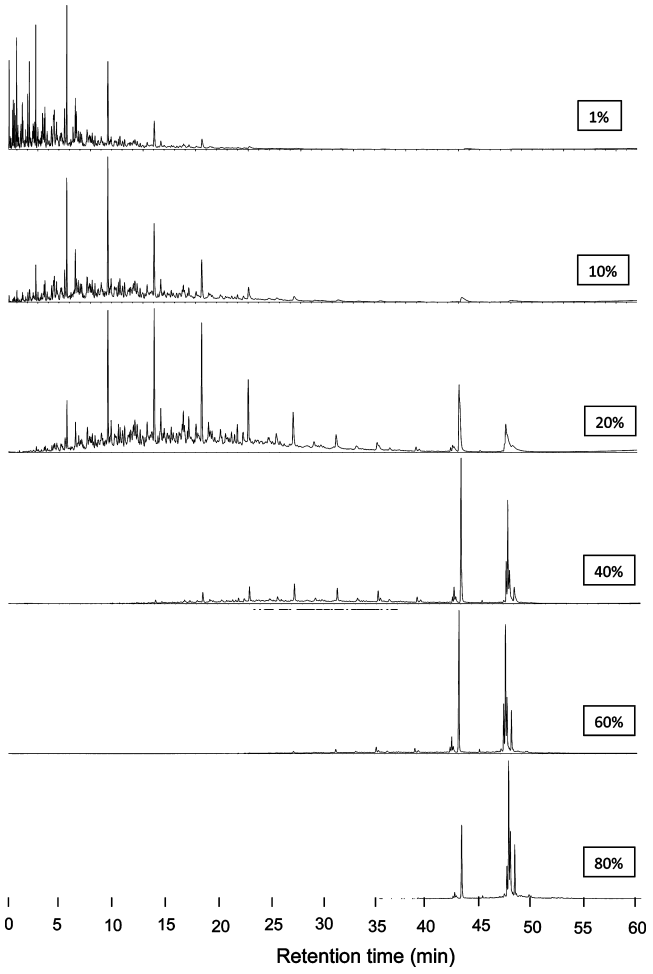

Figure 6. A sequence of the GC-MS chromatograms as function of the volume fraction distilled for diesel fuel−biodiesel fuel blends (20% vol/vol commercial biodiesel fuel).

viscosity and cold flow behavior, the lower molecular mass FAMEs obviously improve these properties.

The CN of a chemical compound depends upon its molecular structure and therefore the fuel composition. As mentioned earlier, the CN increases with an increasing molecular chain length and increasing saturation. Thus, among the main components of a commercial biodiesel fuel, methyl palmitate and methyl stearate have high CNs, while methyl linoleate and methyl linolenate have low CNs (see Table 4). By decreasing the amount of the latter FAMEs in a biodiesel fuel by SCTE at high temperatures, the CN of the fuel can be significantly improved, as shown in Table 4.

The heat of combustion is not a major issue when analyzing the fatty esters most suitable for biodiesel. The data available show that the heat of combustion is in a relatively narrow range between approximately 36 600 and 40 300 kJ/kg for compounds ranging from methyl decanoate to ethyl oleate.[15]

■ CONCLUSIONS

Volatility evaluation with the advanced distillation curve method demonstrates that renewable biodiesel fuel samples obtained from supercritical fluid processing exhibit higher volatility compared to commercial biodiesel fuels produced by the conventional catalytic TE method. Indeed, this volatility is very close to that of the #2 diesel fuel at the start of

dx.doi.org/10.1021/ef300615r | Energy Fuels 2012, 26, 5256−5264

Table 4. Cetane Numbers of Biodiesel Fuel Samples from Chicken Fat and Soybean Oil Obtained by SCTE Compared to Those of a Commercial Biodiesel Fuel Obtained by Catalytic TE (CATTE)[a]

			chicken fat biodiesel fuel (SCTE)			soybean biodiesel fuel (SCTE)			commercial biodiesel fuel (CATTE)		
FAMEs	CN[b]	CN[c]	% vol/vol	CN_{bl}[b]	CN_{bl}[c]	% vol/vol	CN_{bl}[b]	CN_{bl}[c]	% vol/vol	CN_{bl}[b]	CN_{bl}[c]
$C_6H_{12}O_2$		22.85	0.06		0.01						
$C_6H_{10}O_2$			0.02								
$C_7H_{14}O_2$	21.00	28.05	0.18	0.04	0.05						
$C_7H_{12}O_2$			0.05								
$C_8H_{16}O_2$	33.50	33.26	0.45	0.15	0.15	0.82	0.27	0.27			
$C_8H_{14}O_2$			0.28								
$C_9H_{18}O_2$	33.60	38.46	0.41	0.14	0.16	0.78	0.26	0.30			
$C_9H_{16}O_2$			0.11								
$C_{10}H_{20}O_2$		43.67	0.24		0.10						
$C_{10}H_{18}O_2$			0.12								
$C_{11}H_{22}O_2$	47.55	48.87	0.23	0.11	0.11						
$C_{11}H_{20}O_2$			0.07								
$C_{12}H_{24}O_2$	55.60	54.08	0.09	0.05	0.05						
$C_{12}H_{22}O_2$			0.47								
$C_{13}H_{26}O_2$	61.48	59.28	0.08	0.05	0.05						
$C_{13}H_{24}O_2$			0.09								
$C_{14}H_{28}O_2$	73.00	64.49	0.05	0.04	0.03						
$C_{14}H_{26}O_2$			0.03								
$C_{15}H_{30}O_2$	70.57	69.69	0.49	0.34	0.34						
$C_{15}H_{28}O_2$			0.15								
$C_{16}H_{32}O_2$		74.90	0.08		0.06						
$C_{16}H_{30}O_2$			0.05								
$C_{17}H_{34}O_2$	81.08	80.10	23.01	18.66	18.43	23.72	19.23	19.00	13.34	10.82	10.69
$C_{17}H_{32}O_2$	51.00	51	4.39	2.24	2.24	1.27	0.65	0.65			
$C_{18}H_{36}O_2$		85.30	0.16		0.14						
$C_{18}H_{34}O_2$			0.08								
$C_{19}H_{38}O_2$	88.90	90.51	7.63	6.78	6.91	13.4	11.91	12.13	8.62	7.66	7.80
$C_{19}H_{36}O_2$	62.30	62.30	36.12	22.50	22.50	43.29	26.97	26.97	25.92	16.15	16.15
$C_{19}H_{34}O_2$	42.12	42.12	16.92	7.13	7.13	13.74	5.79	5.79	41.51	17.48	17.48
$C_{19}H_{32}O_2$	22.70	22.70	2.00	0.45	0.45	1.04	0.24	0.24	6.47	1.47	1.47
$C_{21}H_{42}O_2$	100.00	95.71	1.16	1.16	1.11						
$C_{22}H_{44}O_2$		100.92	0.28		0.28	1.09		1.10	0.81		0.82
$C_{23}H_{46}O_2$		106.12	0.17		0.18	0.85		0.90	1.55		1.64
CN_{fuel}				59.84[d]	60.49[d]		65.32	67.34		53.58	56.05

[a]A discussion of the uncertainties in the CNs is provided in the references. [b]CN from ref 55. [c]CN calculated by fitting data from ref 55 ($CN_i = 5.2045n_C - 8.3766$, $R^2 = 0.9871$); CN_{bl}[a] − CN of a component blended in the fuel with data from ref 55 CN_{bl}[a] − CN of a component blended in the fuel with fitted data from ref 55. [d]A total HC contribution of 0.54 has to be added.

vaporization, while commercial biodiesel fuel starts boiling at a temperature higher by more than 100 °C.

Analysis by gas chromatography (with mass spectrometry) confirmed that the sample decomposition during distillation. Furthermore, this analysis provided additional insight into the decomposition process and the resulting products of distillation. The distillation curve of the commercial biodiesel fuel exhibits a sharp increase in temperature at volumetric fractions higher than ∼70% as a result of significant thermal decomposition. This phenomenon occurs for the SCTE processed biodiesel fuels beyond 80% distilled fuel.

In addition to the improved volatility, biodiesel fuels obtained by a SCTE process at 400 °C also exhibit higher cetane numbers compared to conventional catalytic biodiesel fuels. Contrary to the current mainstream of anecdotal knowledge, this improvement is due to the beneficial thermal decomposition of the unsaturated FAMEs with low cetane numbers to lower molecular esters and normal hydrocarbons. The increase in overall cetane number is due to a change in fuel composition.

AUTHOR INFORMATION

Corresponding Author

*Email: ganitesc@syr.edu; bruno@boulder.nist.gov.

Notes

The authors declare no competing financial interest.

ACKNOWLEDGMENTS

One of the authors (G.A.) acknowledges the American Recovery and Reinvestment Act for providing financial support.

REFERENCES

(1) Knothe, G.; J. van Gerpen, Krahl, J. *The Biodiesel Handbook*; American 996 Oil Chemists' Society (AOCS) Press: Champaign, IL, 2005.

(2) Sawangkeaw, R.; Bunyakiat, K.; Ngamprasertsith, S. A review of laboratory-scale research on lipid conversion to biodiesel with supercritical methanol (2001−2009). *J. Supercrit. Fluids* **2010**, *55*, 1−13.

(3) Pinnarat, T.; Savage, P. E. Assessment of noncatalytic biodiesel synthesis using supercritical reaction conditions. *Ind. Eng. Chem. Res.* **2008**, *47*, 6801−6808.
(4) Anitescu, G.; Bruno, T. J. Fluid properties needed in supercritical transesterification of triglyceride feedstocks to biodiesel fuels for efficient and clean combustion—A review. *J. Supercrit. Fluids* **2012**, *63*, 133−149.
(5) Anitescu, G.; Bruno, T. J. Liquid biofuels: Fluid properties to optimize feedstock selection, processing, refining/blending, storage/transportation, and combustion. *Energy Fuels* **2012**, *26*, 324−348.
(6) Lee, J.-S.; Saka, S. Biodiesel production by heterogeneous catalysts and supercritical technologies. *Bioresour. Technol.* **2010**, *101*, 7191−7200.
(7) West, A. H.; Posarac, D.; Ellis, N. Assessment of four biodiesel production processes using HYSYS.Plant. *Bioresour. Technol.* **2008**, *99*, 6587−6601.
(8) Huber, G. W.; Iborra, S.; Corma, A. Synthesis of transportation fuels from biomass: Chemistry, catalysts, and engineering. *Chem. Rev.* **2006**, *106*, 4044−4098.
(9) Alleman, T.A.; Fouts, L.; McCormick, R.L. *Analysis of Biodiesel Blend Samples Collected in the United States in 2008*, Technical Report NREL/TP-540−46592; National Renewable Energy Laboratory: Golden, CO, March 2010.
(10) Anitescu, G.; Deshpande, A.; Tavlarides, L. L. Integrated technology for supercritical biodiesel production and power cogeneration. *Energy Fuels* **2008**, *22*, 1391−1399.
(11) Deshpande, A.; Anitescu, G.; Tavlarides, L. L. Supercritical biodiesel production and power cogeneration: Technical and economic feasibilities. *Bioresour. Technol.* **2009**, *101*, 1834−1843.
(12) Marulanda, V.; Anitescu, G.; Tavlarides, L. L. Investigations on supercritical transesterification of chicken fat for biodiesel production from low-cost lipid feedstocks. *J. Supercrit. Fluids* **2010**, *54*, 53−60.
(13) Marulanda, V.; Anitescu, G.; Tavlarides, L. L. Biodiesel fuels through a continuous flow process of chicken fat supercritical transesterification. *Energy Fuels* **2009**, *24*, 253−260.
(14) Glisic, S. B.; Skala, D. U. Phase transition at subcritical and supercritical conditions of triglycerides methanolysis. *J. Supercrit. Fluids* **2010**, *54*, 71−80.
(15) Knothe, G. Designer" biodiesel: Optimizing fatty ester composition to improve fuel properties. *Energy Fuels* **2008**, *22*, 1358−1364.
(16) McCormick, R. L.; Graboski, M. S.; Alleman, T. L.; Herring, A. M.; Tyson, K. S. Impact of biodiesel source material and chemical structure on emissions of criteria pollutants from a heavy-duty engine. *Environ. Sci. Technol.* **2001**, *35*, 1742−1747.
(17) Waynick, J.A. *Characterization of Biodiesel Oxidation and Oxidation Products: CRC Project No. AVFL-2b*, NREL/TP-540−39096; National Renewable Energy Laboratory: Golden, CO, 2005.
(18) DEER Annual Conferences: http://www1.eere.energy.gov/vehiclesandfuels/resources/proceedings/index.html (retrieved 1/7/2012).
(19) Fisher, B. T.; Knothe, G.; Mueller, C. J. Liquid-phase penetration under unsteady in-cylinder conditions: soy- and cuphea-derived biodiesel fuels versus conventional diesel. *Energy Fuels* **2010**, *24*, 5163−5180.
(20) Cheng, A. S.; Fisher, B. T.; Martin, G. C.; Mueller, C. J. Effects of fuel volatility on early direct-injection, low-temperature combustion in an optical diesel engine. *Energy Fuels* **2010**, *24*, 1538−1551.
(21) Anitescu, G. Supercritical fluid technology applied to the production and combustion of diesel and biodiesel fuels. Ph.D. Thesis, Syracuse University, 2008.
(22) Anitescu, G.; Tavlarides, L. L.; Geana, D. Phase transitions and thermal behavior of fuel−diluent mixtures. *Energy Fuels* **2009**, *23*, 3068−3077.
(23) Pitz, W. J.; Mueller, C. J. Recent progress in the development of diesel surrogate fuels. *Prog. Energy Combust. Sci.* **2011**, *37*, 330−350.
(24) Smith, B. L.; Ott, L. S.; Bruno, T. J. Composition-explicit distillation curves of commercial biodiesel fuels: comparison of petroleum derived fuel with B20 and B100. *Ind. Eng. Chem. Res.* **2008**, *47*, 5832−5840.
(25) Bruno, T. J. Improvements in the measurement of distillation curves—Part 1: A composition-explicit approach. *Ind. Eng. Chem. Res.* **2006**, *45*, 4371−4380.
(26) Bruno, T. J. Method and apparatus for precision in-line sampling of distillate. *Sep. Sci. Technol.* **2006**, *41*, 309−314.
(27) Bruno, T. J.; Smith, B. L. Enthalpy of combustion of fuels as a function of distillate cut: Application of an advanced distillation curve method. *Energy Fuels* **2006**, *20*, 2109−2116.
(28) Ott, L. S.; Smith, B. L.; Bruno, T. J. Composition-explicit distillation curves of mixtures of diesel fuel with biomass-derived glycol ester oxygenates: A fuel design tool for decreased particulate emissions. *Energy Fuels* **2008**, *22*, 2518−2526.
(29) Ott, L. S.; Bruno, T. J. Variability of biodiesel fuel and comparison to petroleum-derived diesel fuel: Application of a composition and enthalpy explicit distillation curve method. *Energy Fuels* **2008**, *22*, 2861−2868.
(30) Huber, M. L.; Lemmon, E.; Kazakov, A.; Ott, L. S.; Bruno, T. J. Model for the thermodynamic properties of a biodiesel fuel. *Energy Fuels* **2009**, *23*, 3790−3797.
(31) Bruno, T. J.; Ott, L. S.; Smith, B. L.; Lovestead, T. M. Complex fluid analysis with the advanced distillation curve approach. *Anal. Chem.* **2010**, *82*, 777−783.
(32) Bruno, T. J.; Ott, L. S.; Lovestead, T. M.; Huber, M. L. The composition explicit distillation curve technique: relating chemical analysis and physical properties of complex fluids. *J. Chromatogr. A* **2010**, *1217*, 2703−2715.
(33) Bruno, T. J.; Ott, L. S.; Lovestead, T. M.; Huber, M. L. Relating complex fluid composition and thermophysical properties with the advanced distillation curve approach. *Chem. Eng. Technol.* **2010**, *33*, 363−376.
(34) Bruno, T. J.; Lovestead, T. M.; Huber, M. L. Prediction and preliminary standardization of fire debris analysis constituents with the advanced distillation curve method. *J. Forensic Sci.* **2011**, *56*, S191−S202.
(35) Bruno, T.J.; Svoronos, P.D.N. *CRC Handbook of Fundamental Spectroscopic Correlation Charts*; Taylor and Francis CRC Press: Boca Raton, FL, 2006.
(36) Bruno, T.J.; Svoronos, P.D.N. *CRC Handbook of Basic Tables for Chemical Analysis*, 3rd ed.; Taylor and Francis CRC Press: Boca Raton, FL, 2011.
(37) *NIST/EPA/NIH Mass Spectral Database*, SRD Program;National Institute of Standards and Technology: Gaithersburg, MD, 2005.
(38) Lovestead, T. M.; Windom, B. C.; Bruno, T. J. Investigating the unique properties of Cuphea-derived biodiesel fuel with the advanced distillation curve method. *Energy Fuels* **2010**, *24*, 3665−3675.
(39) Bruno, T. J.; Smith, B. L. Improvements in the measurement of distillation curves—Part 2: Application to aerospace/aviation fuels RP-1 and S-8. *Ind. Eng. Chem. Res.* **2006**, *45*, 4381−4388.
(40) Smith, B. L.; Bruno, T. J. Improvements in the measurement of distillation curves—Part 3: Application to gasoline and gasoline + methanol mixtures. *Ind. Eng. Chem. Res.* **2007**, *46*, 297−309.
(41) Smith, B. L.; Bruno, T. J. Improvements in the measurement of distillation curves—Part 4: Application to the aviation turbine fuel Jet-A. *Ind. Eng. Chem. Res.* **2007**, *46*, 310−320.
(42) Windom, B. C.; Bruno, T. J. Improvements in the measurement of distillation curves—Part 5: Reduced pressure distillation curve method. *Ind. Eng. Chem. Res.* **2011**, *50*, 1115−1126.
(43) Tang, H.; Salley, S. O.; Simon Ng, K. Y. Fuel properties and precipitate formation at low temperature in soy-, cottonseed-, and poultry fat-based biodiesel blends. *Fuel* **2008**, *87*, 3006−3017.
(44) Seames, W.; Luo, W.; Ahmad, I.; Aulich, T.; Kubatova, A.; Stavova, J.; Kizliak, E. The thermal cracking of canola and soybean methyl esters: improvement of cold flow properties. *Biomass Bioenergy* **2010**, *34*, 939−946.

(45) Luo, W.; Ahmad, I.; Kubatova, A.; Stavova, J.; Aulich, T.; Sadrameli, S. M.; Seames, W. The thermal cracking of soybean/canola oils and their methyl esters. *Fuel Process. Technol.* **2010**, *91*, 613−617.
(46) Wexler, H. Polymerization of drying oils. *Chem. Rev.* **1964**, *64*, 591−611.
(47) Windom, B. C.; Bruno, T. J. Pressure-controlled advanced distillation curve analysis of biodiesel fuels: analysis of thermal decomposition. *Energy Fuels* **2011**, submitted.
(48) Andersen, W. C.; Bruno, T. J. Thermal decomposition kinetics of RP-1 rocket propellant. *Ind. Eng. Chem. Res.* **2005**, *44*, 1670−1676.
(49) Andersen, W. C.; Bruno, T. J. Rapid screening of fluids for chemical stability in organic Rankine cycle applications. *Ind. Eng. Chem. Res.* **2005**, *44*, 5560−5566.
(50) Widegren, J. A.; Bruno, T. J. Thermal decomposition kinetics of the aviation fuel Jet-A. *Ind. Eng. Chem. Res.* **2008**, *47*, 4342−4348.
(51) Widegren, J.A.; Bruno, T.J. Thermal decomposition of RP-1 and RP-2, and mixtures of RP-2 with stabilizing additives. *Proceedings of the 4th Liquid Propulsion Subcommittee, JANNAF*, Dec. 2008.
(52) Widegren, J. A.; Bruno, T. J. Thermal decomposition kinetics of propylcyclohexane. *Ind. Eng. Chem. Res.* **2009**, *48*, 654−659.
(53) Widegren, J. A.; Bruno, T. J. Thermal decomposition kinetics of the kerosene based rocket propellants 2. RP-2 stabilized with three additives. *Energy Fuels* **2009**, *23*, 5523−5528.
(54) Widegren, J. A.; Bruno, T. J. Thermal decomposition kinetics of kerosene-based rocket propellants. 1. Comparison of RP-1 and RP-2. *Energy Fuels* **2009**, *23*, 5517−5522.
(55) Murphy, M.J.; Taylor, J.D.; McCormick, R.L. *Compendium of Experimental Cetane Number Data*, Technical Report NREL/SR-540-36805; National Renewable Energy Laboratory: Golden, CO, Sept. 2004.